MODIFICATION OF IONOTROPIC GLUTAMATE RECEPTOR–MEDIATED PROCESSES IN THE RAT HIPPOCAMPUS FOLLOWING REPEATED, BRIEF SEIZURES

S. BORBÉLY,[a]* E. DOBÓ,[b] D. CZÉGÉ,[a] E. MOLNÁR,[c]
M. BAKOS,[b] B. SZŰCS,[b] A. VINCZE,[b] I. VILÁGI[a]
AND A. MIHÁLY[b]

[a]*Department of Physiology and Neurobiology, Eötvös Loránd University, H-1117, Budapest Pázmány Péter sétány 1/C, Hungary*

[b]*Department of Anatomy, Faculty of Medicine, University of Szeged, Szeged, Hungary*

[c]*MRC, Centre for Synaptic Plasticity, Department of Anatomy, School of Medical Sciences, University of Bristol, Bristol, UK*

Abstract—The seizure-induced molecular and functional alterations of glutamatergic transmission in the hippocampus have been investigated. Daily repeated epileptic seizures were induced for 12 days by intraperitoneal administration of 4-aminopyridine (4-AP; 4.5 mg/kg) in adult Wistar rats. The seizure symptoms were evaluated on the Racine's scale. One day after the last injection, the brains were removed for *in vitro* electrophysiological experiments and immunohistochemical analysis. The glutamate receptor subunits NR1, NR2A, NR2B, GluR1, GluR1$_{flop}$, GluR2, and KA-2 were studied using the histoblotting method. The semi-quantitative analysis of subunit immunoreactivities in hippocampal layers was performed with densitometry. In the hippocampus, increase of GluR1, GluR1$_{flop}$ and NR2B immunostaining was observed in most of the areas and layers. The significant decrease of GluR2 staining intensity was observed in the CA1 and dentate gyrus. Calcium permeability of hippocampal neurons was tested by a cobalt uptake assay in hippocampal slices. The uptake of cobalt increased in the CA1 area and dentate gyrus, but not in the CA3 region following 4-AP treatment. Effects of AMPA and NMDA (*N*-methyl-D-aspartate) glutamate receptor antagonists (1-(4-aminophenyl)-4-methyl-7,8-methylenedioxy-5H-2,3-benzodiazepine hydrochloride (GYKI 52466) and D-APV respectively) were measured in hippocampal slices using extracellular recording. Analysis of the population spikes revealed the reduced effectiveness of the AMPA receptor antagonist GYKI 52466, while the effect of the NMDA receptor antagonist D-(2R)-amino-5-phosphonovaleric acid was similar to controls. The results demonstrated that repeated convulsions induced structural and functional changes in AMPA receptor–mediated transmission, while NMDA and kainate receptor systems displayed only alterations in receptor subunit composition. © 2009 IBRO. Published by Elsevier Ltd. All rights reserved.

*Corresponding author. Tel: +36-1-209-0555-8391; fax: +36-1-381-2182.
E-mail address: bosa@ludens.elte.hu (S. Borbély).

Key words: brain slice, 4-aminopyridine, histoblot, Co^{2+}-uptake, electrophysiology, subunit composition, glutamate antagonists.

Human epilepsy, due to the chronic, recurrent convulsive states, causes a slowly ongoing neuronal degeneration in the most involved brain structures: allocortex, neocortex and diencephalon (Honavar et al., 2002). The main cause of neuronal death is the excessive release and excitotoxicity of glutamate and aspartate and the hypoxia of the convulsing brain (Meldrum and Nilsson, 1976; Sloviter and Dempster, 1985; Pena and Tapia, 2000). In human case histories, very often the first symptom towards a long-lasting pathological change is the acute convulsion—therefore modeling of the effects of repeated acute seizures may provide important information about the pathogenesis of epilepsy.

Chronic animal models such as pilocarpine- (Turski et al., 1983) or kainic acid− (Nadler et al., 1978) induced status epilepticus result in neurodegeneration in the hippocampus, neocortex, amygdala, substantia nigra and thalamus (Berg et al., 1993; Cavalheiro, 1995; Singh et al., 1991; Turski et al., 1983). Neuronal degeneration leads to deafferentation of other neuronal assemblies, and the formation of pathological neuronal circuits, which in turn result in secondary generalized seizures (Michaelis, 1998). Our previous studies revealed that low doses of 4-aminopyridine (4-AP) precipitated acute behavioral convulsions in experimental animals, and these convulsions were accompanied by characteristic temporary pathophysiological phenomena: large increase of transmitter release (Kovács et al., 2003), enhancement of cerebral blood flow (Fabene et al., 2006; Mihály et al., 2000) and the appearance of c-fos protein in the cell nucleus of the neurons (Mihály et al., 2001; Szakács et al., 2003). We also proved that the behavioral symptoms and the neuronal c-fos expression could be prevented by the application of *N*-methyl-D-aspartate (NMDA) receptor antagonists, indicating the activation and role of ionotropic glutamate receptors (iGluRs; Szakács et al., 2003). On the other hand, no neuronal degeneration or other long-lasting tissue damage was detected following administration of low doses of 4-AP (Fabene et al., 2006; Vizi et al., 2004).

Regulation of iGluR subunits is complex, including several intracellular steps, from gene expression to post-translational modifications (Hassel and Dingledine, 2006). Previous studies indicate the importance of iGluR subunit composition in different experimental epilepsies (Porter et

al., 2006). We aimed to reveal the changes in subunit composition of iGluRs using a semi-quantitative immunohistoblot method. Similarly, we studied changes in general excitability and pharmacological sensitivity of NMDA and AMPA receptors in hippocampal slices in electrophysiological experiments, to gain information about functional consequences of repeated seizures and the possible receptor subunit rearrangement. Cobalt crosses the cell membrane through Ca^{2+}-permeable, ligand-gated non-NMDA glutamate receptors. Therefore, we also investigated possible changes in Ca^{2+} permeability of hippocampal neurons using an *in vitro* cobalt uptake assay of brain slices from control and 4-AP-treated rats.

EXPERIMENTAL PROCEDURES

Experiments were performed on adult, male Wistar rats (150–280 g, Charles River, Hungary). All experiments were approved by the Regional Animal Care Committees and by the Budapest Animal Health Care Authority. Rats were kept under constant 12-h light/dark cycle and controlled temperature (22 ± 2 °C). Standard pellet food and tap water were available *ad libitum*.

Treatment of animals

Rats received i.p. 4-AP injections during 12 consecutive days. The starting dose was 4.5 mg/kg. After the first 3 days, in case of those rats which failed to produce stage 5 seizures according to the Racine-type scale (Racine, 1972), the dose was increased by 5%, and it was further increased by 5% steps if stage 5 seizures failed to develop at the previous day. The upper limit of dose was 6.65 mg/kg. Control rats received daily i.p. physiological saline for 12 days.

Histoblot analysis of iGluR proteins

Rats were sacrificed on day 13 of the experiment (after daily treatment with 4-AP for 12 days), to determine changes in the densities of AMPA, NMDA and kainate (KA) type iGluR subunit proteins, using an *in situ* blotting technique (histoblot, Tonnes et al., 1999; Kopniczky et al., 2005). In brief, animals were deeply anesthetized with diethyl ether, decapitated, and the brains were quickly frozen in isopentane and stored at −80 °C until sectioning. Horizontal plane cryostat sections (10 μm) were cut and mounted on glass slides. Small, rectangular pieces of nitrocellulose membrane (Schleicher & Schuell, BA85, 0.45 μm), were moistened with 48 mM Tris-base, 39 mM glycine, 2% (w/v) SDS and 20% (w/v) methanol for 15 min at room temperature. The glass slide with the tissue section facing down was placed on the membrane, and gently pressed for 30 seconds. The membrane was taken from the glass slide, and used for the immunoblotting. After blocking in 5% (w/v) non-fat dry milk in PBS, nitrocellulose membranes were DNase I-treated (5 U/ml), washed and incubated in 2% (w/v) SDS, 100 mM β-mercaptoethanol in 100 mM Tris–HCl (pH 7.0), for 60 min at 45 °C to remove adhering tissue residues. After excessive washing, blots were reacted with affinity-purified subunit specific antibodies in blocking solution overnight, at 4 °C. The following primary antibodies were used: anti-GluR2 (Chemicon; 1 μg/ml); anti-GluR1-4 (pan-AMPA, Pickard et al., 2000); anti-GluR1flop (2 μg/ml; Tonnes et al., 1999); anti-NR1 (PharMingen; 2 μg/ml); anti-NR2A (Chemicon; 1 μg/ml); anti-NR2B (Molecular Probes; 0.2 μg/ml); anti-KA-2 (Upstate; 1:500). The bound primary antibodies were labeled with alkaline phosphatase-conjugated antirabbit IgG secondary antibody (1:500; Promega, USA). The enzyme was visualized in a developer containing 0.33% Nitro Blue Tetrazolium, 0.66% 5-bromo-4-chloro-3-indolyl phosphate in 70% dimethyl-formamide Chemicals for histoblotting (where not

indicated) were purchased from Sigma. To facilitate the identification of structures and cell layers, adjacent cryostat sections were stained with Cresyl Violet. Digital images were acquired by scanning the membranes using a desktop scanner. Image analysis and processing were performed using the Adobe Photoshop® software (Adobe Systems, San Jose, CA, USA). When processing, the images were treated identically to allow comparison. Pixel density was determined for different hippocampal regions. The pixel density of immunoreactivity was measured by an experimenter blind to the experimental conditions using a previously established quantification strategy (Xu et al., 2004; Kopniczky et al., 2005). Briefly: open circular cursors with a diameter of 0.10 mm were placed at adjacent positions along the stratum oriens (eight circles), stratum radiatum (six circles), stratum lacunosum moleculare (seven circles), stratum moleculare of DG (12 circles), hilum of DG (six circles) and stratum lucidum of CA3 (seven circles; as illustrated on Fig. 1). The average of 10 background determinations (carried out near the brain protein–containing areas of the immunostained nitrocellulose papers) was subtracted from the average pixel densities measured within various hippocampal regions. Following background corrections, the average pixel density for the whole subregion of the hippocampus from one animal counted as one "*n*." Data were analyzed and plotted using a GraphPad® version 4.0. Differences between the corresponding hippocampal regions were assessed using a two-way analysis of variance (ANOVA), and further compared with the Bonferroni post hoc test, at a minimum confidence level of $P<0.05$. The number of animals was five to seven in every experimental group. We prepared 20–36 blots (equal to the number of cryostat sections used for blotting) for each antibody. This number is seen in Fig. 1 as the "*n*" value.

Cobalt-uptake determination

Following the daily 4-AP injections (on day 13), 9 control and 10 4-AP-treated animals were sacrificed and 250 μm thick hippocampal slices were prepared to study Co^{2+} uptake. From each Animal eight to 20 slices were stained and evaluated successfully. The procedure was performed as described previously (Pruss et al., 1991). Briefly, the slices were incubated in a Ca^{2+}-free incubation solution for 5 min before placement into an uptake buffer. This buffer contained 13 mM sucrose, 57.5 mM NaCl, 5 mM KCl, 2 mM $MgCl_2$, 1 mM $CaCl_2$, 12 mM glucose, 10 mM Hepes, and, in addition, 5 mM $CoCl_2$ and 100 μM kainate (KA). Incubation lasted for 20 min. Slices incubated in the same solution without KA served as background controls. After the stimulated, Co^{2+} uptake, slices were rinsed once in the uptake buffer and incubated in the same buffer containing 2 mM EDTA to remove non-specifically bound Co^{2+}. Then, slices were rinsed twice in the uptake buffer, and Co^{2+} was precipitated by incubation in 0.12% (w/v) $(NH_4)_2S$ solution for 5 min. During this procedure, dark CoS precipitate was formed in the cells. At the end, slices were fixed in 4% (w/v) paraformaldehyde for 30 min and mounted in glycerin for further computer analysis. The Co^{2+}-stained slices were analyzed with an Olympus CH2 microscope equipped with an Olympus Camedia C4040-Zoom digital camera connected to a PC running an AnalySIS 3.2 Docu (Soft Imaging Systems Gmbh) software. Pictures were digitized at a fourfold magnification and converted to eight bit grey color images. Evaluation of optical density (OD) was performed in every layer of the hippocampal formation (Fig. 2). The average density of a sampling box containing 5000 or 10,000 pixels of the investigated area was determined. In all series of experiments, the difference of mean OD values of sampling areas between untreated and KA-stimulated slices was calculated. Slices from control and 4-AP-treated animals were compared, differences in Co^{2+} uptake were calculated by comparing relative OD values.

Unpaired Student's *t*-test for independent variables was performed on the means of OD values. Homogeneity of variances
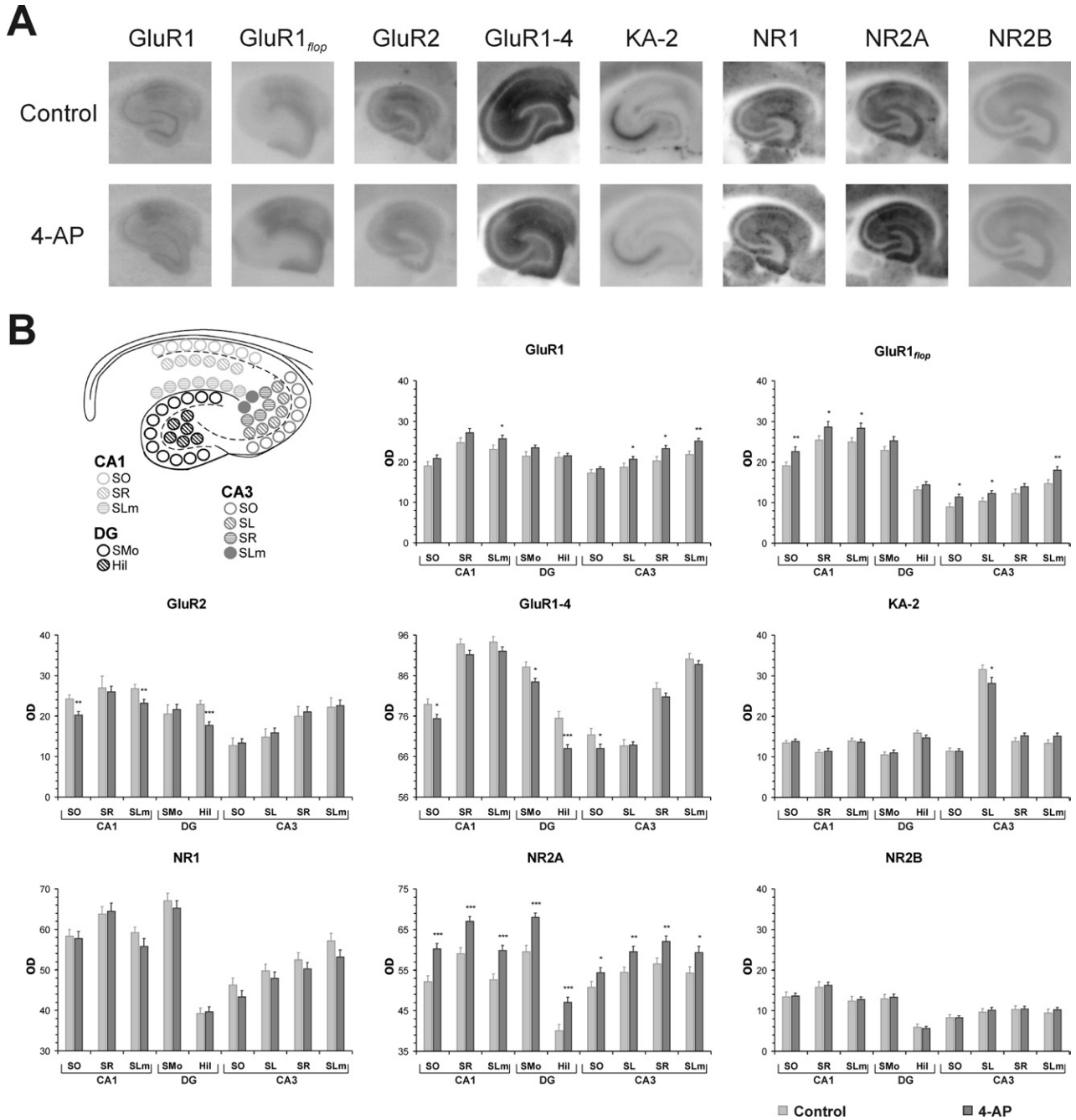
Fig. 1. Sampling areas and changes in the relative density of iGluRs in different hippocampal regions. (A) Representative images of histoblot sections from slices of control and 4-AP-treated animals. (B) Upper left corner demonstrates sampling areas of the hippocampal formation. Graphs indicate alterations in the amount of glutamate receptor subtypes. Decrease of the GluR2 receptor subtype was observed in the hippocampal CA1 and dentate gyrus areas, while an enhanced level of GluR1, GluR1$_{flop}$ and NR2A subtypes was detected in CA1 and CA3 regions. The NR1 receptor subtype was unaffected in all investigated regions. Abbreviations: SO, str. oriens; SR, str radiatum; SLm, str. lacunosum-moleculare; SL, str. lucidum; SMo, str. moleculare; Hil, hilum. * Indicates significant differences at $P < 0.05$, while ** means $P < 0.01$, and *** means $P < 0.001$. The "n" values are as follows: NR1: 24; NR2A: 24; NR2B: 20; GluR1: 26; GluR1-4: 24; GluR1$_{flop}$: 24; GluR2: 20; KA-2: 36 (see also text).

was tested before statistical analysis. Data are presented as mean±standard error of the mean (SEM).

Slice preparation and electrophysiological recording of hippocampal synaptic transmission

Electrophysiological experiments were carried out on 400 μm thick brain slices ($n=64$) originating from 22 rats. The hippocam-

pal slices were prepared 1 day after the last seizure induction (day 13). Rats were decapitated in deep chloral hydrate anesthesia, the brain was quickly removed and horizontal slices containing the hippocampus, entorhinal and somatosensory cortices were cut with a vibratome. After a 1 h regeneration period in Hepes-buffer (pH: 7.1–7.2)-containing solution, slices were transferred to an Oslo-type recording chamber (FST, Canada) through which stan-
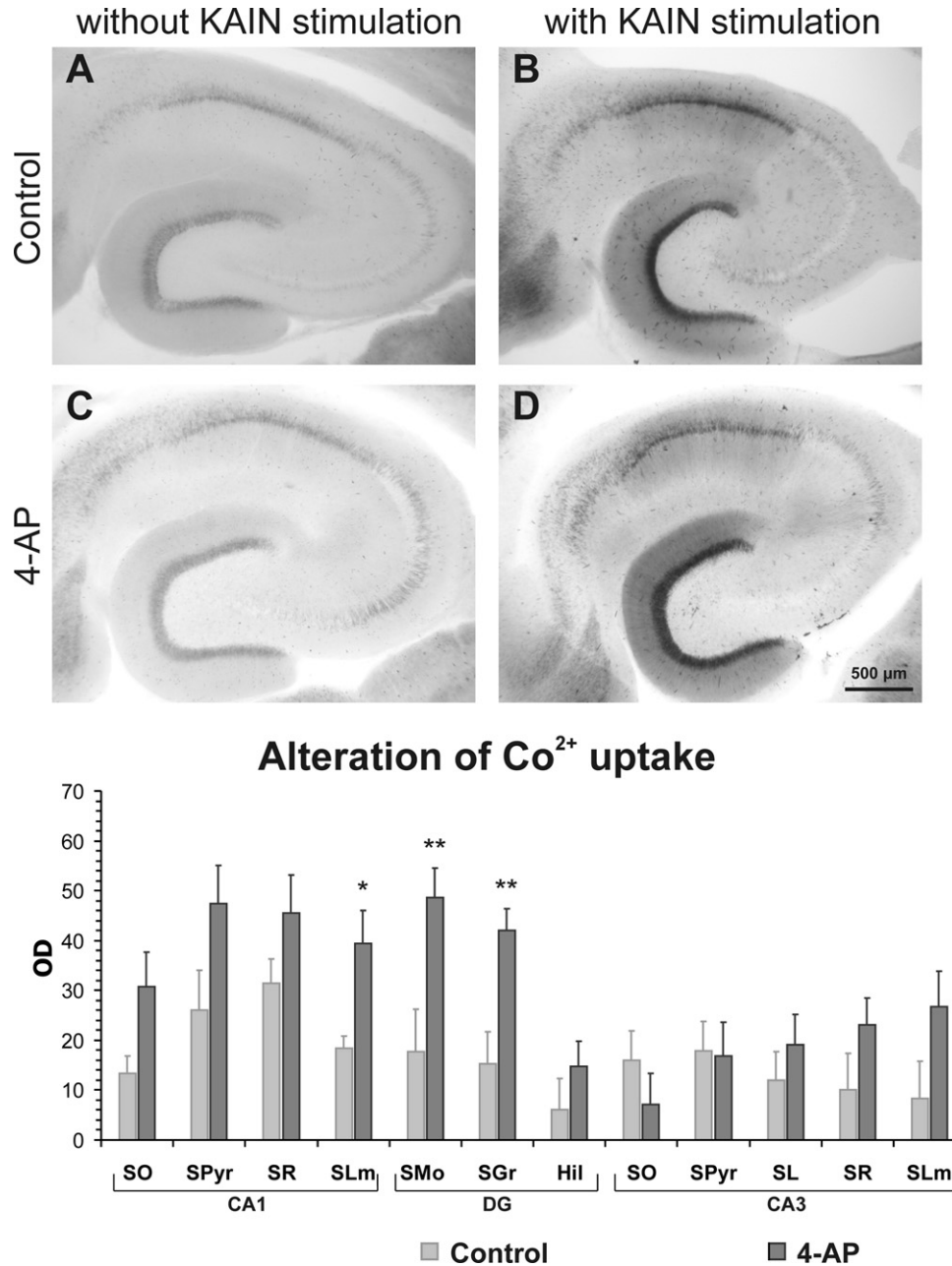
Fig. 2. A characteristic pattern of Co^{2+} uptake measurement and results of OD determination. Images are representing histochemical sections for Co^{2+} uptake investigations. Images A and C were taken from control and 4-AP-treated animals, respectively, without kainic acid-facilitation, while images B and D show kainic acid–stimulated sections from the control and the 4-AP group, respectively. The graph shows the changes of Co^{2+} uptake, which is connected to Ca^{2+} permeability of non-NMDA receptors. 4-AP-treated animals showed enhanced Ca^{2+} permeability in the CA1 and dentate gyrus regions. Abbreviations: SO, str. oriens; SR, str. radiatum; SLm, str. lacunosum-moleculare; SL, str. lucidum; SPyr, str. pyramidale; SMo, str. moleculare; SGr, str. granulosum; Hil, hilum. * Indicates significant differences at $P<0.05$, while ** means $P<0.01$.

dard artificial cerebrospinal fluid (ACSF) was perfused (2.5–3 ml/min) using a peristaltic pump (Heidolph PD 5101). The ACSF was saturated with carbogen (95% O_2−5% CO_2) at about 33±1 °C. The composition of this standard perfusion solution was (in mM): 126 NaCl; 26 $NaHCO_3$; 1.8 KCl; 1.25 KH_2PO_4; 1.3 $MgSO_4$; 2.4 $CaCl_2$; 10 glucose.

Glass microelectrodes filled with 1 M NaCl (8–10 MΩ) were positioned as recording electrodes in the stratum pyramidale of the hippocampal CA1 region, while bipolar tungsten stimulating electrodes were positioned at the Schaffer axon collaterals to

evoke population (POP) spikes. Duration of the stimulation square voltage pulses was 100 μs and the amplitude was gradually varied between threshold and supramaximal values. Signals were amplified with an Axoclamp 2 B amplifier (Axon Instruments, Inc., Union City, CA, USA), A/D converted and recorded with the SPEL Advanced Intrasys computer program (Experimetria, Ltd., Budapest, Hungary).

The viability of slices was tested before each experiment. Characteristic field responses were recorded applying single shock stimulation. If POP-spike amplitude at maximum stimulus

intensity was smaller than 3 mV, the slice was excluded from the experiments. Slices were continuously stimulated with medium-strength stimuli at a rate of 0.05 Hz. Fifteen minutes after placing the slices into the recording chamber, the stimulus threshold (T) was determined, and then an input–output (I–O) curve was recorded when gradually increasing the stimulus intensity from 1 to 3 T in 0.25 T steps and response amplitudes were plotted against intensities. At each stimulus intensity mean amplitude values were calculated from three evoked responses. Subsequently, 0.05 Hz continuous stimulation was applied with 2 T if not specified otherwise. Responses evoked at 2 T stimulation intensity were calculated as a mean of 10 evoked responses and called "average response (AR)." Depending on the aim of the actual test, different protocols were performed. In control cases no special achievement was applied. When pharmacological sensitivity of particular glutamate receptors was analyzed, standard perfusion solution was switched either to AMPA-receptor antagonist containing solution (40 μM GYKI 52466 (1-(4-aminophenyl)-4-methyl-7,8-methylenedioxy-5H-2,3-benzodiazepine hydrochloride), or to NMDA receptor antagonist containing solution (25 μM D-APV—(2R)-amino-5-phosphonovaleric acid). Treatment with GYKI 52466 lasted for 30 min, while APV containing solution was perfused until 10 min. Recordings were finished by determination of test responses and I–O curves. Each experimental group contained 8–8 independent records.

Amplitude of the POP-spike and the EPSP slope was analyzed with the SPEL Advanced Intrasys computer program (Experimetria, Ltd.). One-way ANOVA followed by Newman–Keuls post hoc comparison was performed on the means of POP-spike amplitudes. Homogeneity of variances and normal distribution of data were tested before statistical analysis. Data are presented as mean±SEM.

RESULTS

Seizure behavior

Studies on seizure event characteristics were performed on 27 animals, surviving the 12 treatment days. The i.p. administration of 4-AP induced generalized tonic–clonic seizures. On average, two seizures were detected following each treatment. The first seizure event appeared in the first 30 min, which sometimes was followed by a second fit within the first hour after the convulsant treatment. The latency of first tonic–clonic seizure was changing during the repeated 4-AP treatment: five of 27 animals showed decreasing latency, compared to the first one. In five rats proportion of decreased and increased latency times of first seizure events was 50%–50%, while in 17 of 27 animals increased latency was detected. Seizures occurred only within 3 h following 4-AP administration. No spontaneous convulsions were observed. The behavioral symptoms of 4-AP treatment were similar to that described previously (Mihály et al., 1990; Szakács et al., 2003; Weiczner et al., 2008).

Histoblot analysis of iGluR subunits

NMDA receptor subunits. NMDA receptor subunits NR1, NR2A and NR2B are ubiquitous in the hippocampus, and most abundant in the supra- and infrapyramidal layers of the regio superior and the molecular layer of the dentate gyrus. These areas show a much stronger immunostaining than any other forebrain structure. The NR1 subunit staining density did not change at the end of the 2 weeks' 4-AP

treatment. Alterations of the NR2A subunit density were detectable on day 13, when every layer of the CA1 and CA3 regions showed a highly significant increase in staining density (n=20; P<0.001 in CA1; P<0.01 in CA3; Fig. 1). The same alterations were detected in the molecular layer and in the hilum of the dentate gyrus (n=20; P<0.001; Fig. 1). Staining density of the NR2B subunit did not change in any of the hippocampal layers.

AMPA and KA receptor subunits. The AMPA receptors were investigated with pan-AMPA (anti-GluR1-4) antibodies reacting with every subunit, and antibodies specific to GluR1, GluR1$_{flop}$ and GluR2 subunits. In control animals, staining with pan-AMPA antibodies was strong in stratum oriens of CA1, in the suprapyramidal layers of CA1-3 and in the molecular layer of the dentate gyrus. The GluR1 subunit antibody displayed a high staining density in strata oriens, radiatum and lacunosum-moleculare of CA1, and in the outer segment of the dentate molecular layer. The GluR1$_{flop}$ staining was strongest in the strata oriens, radiatum and lacunosum-moleculare of CA1, and in the molecular layer of the dentate gyrus. The GluR2 antibody strongly labeled the stratum lacunosum-moleculare of CA1, CA3, stratum radiatum of CA1, and outer segment of the upper blade of the dentate molecular layer. Immunostaining of the stratum oriens of CA1, the hilum and the lower blade of the dentate molecular layer were weaker. The KA-2 antibody revealed a strong immunoreactivity in the stratum lucidum of CA3.

In convulsing animals, we detected significant decrease of pan-AMPA staining intensity in stratum oriens of CA1-3 (n=24; P<0.05), and in stratum moleculare (P<0.05) and hilum (P<0.001) of the dentate gyrus (n=24; Fig. 1). Significant increase in GluR1 staining was seen in stratum lacunosum-moleculare (P<0.05) of CA1, stratum lucidum (P<0.05) and lacunosum-moleculare (P<0.01) of CA3 (n=26; Fig. 1). The staining with the GluR1$_{flop}$ antibody increased significantly in every area and layer, except the dentate gyrus and the stratum radiatum of CA3 (P<0.05 and 0.01; n=24; see Fig 1). Decrease of GluR2 density was detected in strata oriens and lacunosum-moleculare of CA1 (P<0.01), and hilum of the dentate gyrus (P<0.001) (n=20; Fig. 1). The KA-2 immunostaining in stratum lucidum of the CA3 decreased significantly in the convulsing animals (P<0.05; n=36; Fig. 1).

Modification in Co^{2+} uptake through activated AMPA receptors

OD analysis of KA-induced cobalt uptake in the hippocampus revealed regionally different changes. The CA1 hippocampal area and the dentate gyrus showed increased cobalt uptake compared to controls in most of the investigated layers, while the CA3 region remained unaffected (Fig. 2). Comparison of control (n=9) and 4-AP treated (n=10) slices revealed a significant increase in the amount of cobalt precipitate in strata moleculare (P<0.01) and granulosum (P<0.01) of the dentate gyrus and stratum lacunosum-moleculare (P<0.05) of the CA1 area of the convulsing animals (Fig. 2). Remaining layers of the af-

fected regions also displayed a rise in staining intensity but these increases were not significant.

Modification of hippocampal synaptic transmission

Extracellular evoked field potential recordings were obtained from horizontal brain slices, including the hippocampus. Amplitude of POP-spikes and slope of EPSPs were evaluated.

General neuronal excitability. Spontaneous discharges were not detected in the control and in the 4-AP-treated slices. Threshold of evoked response was determined at the beginning of experiments. The mean intensity was 3.1±0.07 V ($n=32$) in control slices, and 3.0±0.10 V ($n=32$) in 4-AP-treated slices, this difference was not significant ($P=0.26$). Following the determination of stimulus threshold (T), POP-spike amplitude was measured to test the general excitability. In each case a stimulus intensity–evoked response (I–O) curve was recorded (Fig. 3, left panel), amplitude values were averaged and plotted at all stimulus intensities in control and 4-AP-treated slices. The mean of the POP-spike amplitudes at 2 T was 6.0±0.4 mV ($n=32$) in slices of control animals, and 7.3±0.5 mV ($n=32$) in slices of 4-AP-treated animals. The pattern of the evoked responses was similar in both groups. Data evaluation revealed a significant increase of general excitability up to 2.25 T stimulus intensity, with an average rise of 30.0%±5.3% following 4-AP treatment.

Analysis of pre- and postsynaptic effects of 4-AP treatment on the postsynaptic current is based on the method described by Wheal et al. (1998). Briefly, the slope of POP spike is in correlation with the extracellular field (E) generated by a post-synaptic current, while the amplitude of a POP spike (S) represents the probability of action potential generation in the postsynaptic neurons. Distinct separation of data from experimental groups of animals was observed (E/S curve; Fig. 3, right panel), repetitive seizure induction resulted in an E/S potentiation (left shift) in treated rats.

In contrast to the above findings, the average threshold of hippocampal POP-spike did not change (3.1±0.7 V; $n=32$ and 3.1±0.10 V; $n=32$ in control and 4-AP group, respectively; $P>0.05$).

Pharmacological sensitivity to AMPA and NMDA receptor antagonists. A mild facilitation was observed both in control and in 4-AP-treated groups during the 30 min incubation in ACSF, which was presumably due to the recording protocol: the amplitude of evoked POP spikes was enhanced during the 10 or 30 min of low-frequency stimulation. This increment was relatively smaller in the slices originating from 4-AP-treated rats.

In the control hippocampi at a stimulus intensity of 2 T, the relative POP-spike amplitude was 92%±1.8% ($n=8$) of the maximal amplitude, which increased to 185%±13.8% ($n=8$) after 30 min incubation time (Fig. 4). In slices of 4-AP-treated animals the basic value was 91%±0.9% ($n=8$), which changed to 160%±9.0% ($n=8$) in ACSF perfusion. The AMPA receptor antagonist GYKI 52466 effectively decreased this enhancement in both groups at each stimulus intensities. GYKI 52466 exerted a stronger inhibition in control slices: at 2 T stimulus intensity, the relative amplitude of the POP-spike was only 29%±6.9% ($n=8$). In hippocampi of the 4-AP-treated rats this antagonism was smaller: the amplitude of the POP-spike reached 74%±5.5% ($n=8$) of the maximal amplitude (Fig. 4A, B). Further consequence of the 4-AP treatment was that the dynamics of synaptic transmission saturation changed: the antagonist was more effective at lower stimulus intensities (Fig. 4C).

Statistical comparison of the decreases of the POP-spike amplitude caused by GYKI 52466 also revealed a significant difference between control and 4-AP-treated rats (* $P=0.0214$). GYKI 52466 treatment resulted in a strong E/S depression (right shift) which means the reduction of POP-spike amplitude (*** $P=0.00018$) without the alteration of EPSP slope ($P=0.263$) in control rats, while in 4-AP-treated animals decrease of both the POP-spike am-
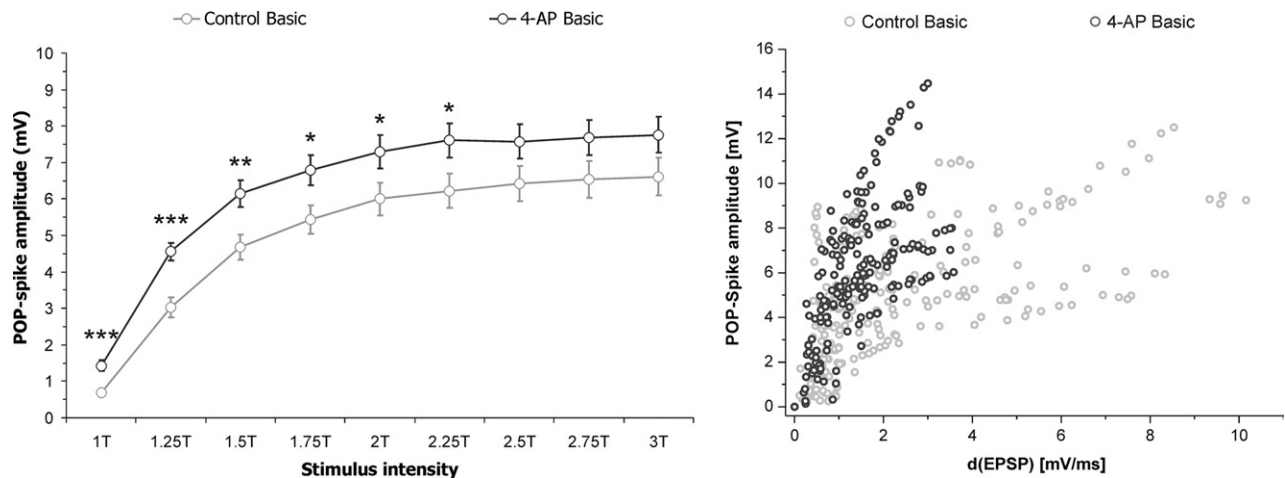

Fig. 3. Alteration of basic excitability in different treatment groups. At each stimulus intensity, basic activity in slices from 4-AP-treated animals showed a general enhancement compared to the control (left panel). According to E/S curve (right panel) a mild E/S potentiation (left shift) has occurred in the 4-AP group. dEPSP means slope (or derivative) of EPSP. * Indicates significant differences at $P<0.05$, while ** means $P<0.01$, and *** means $P<0.001$.
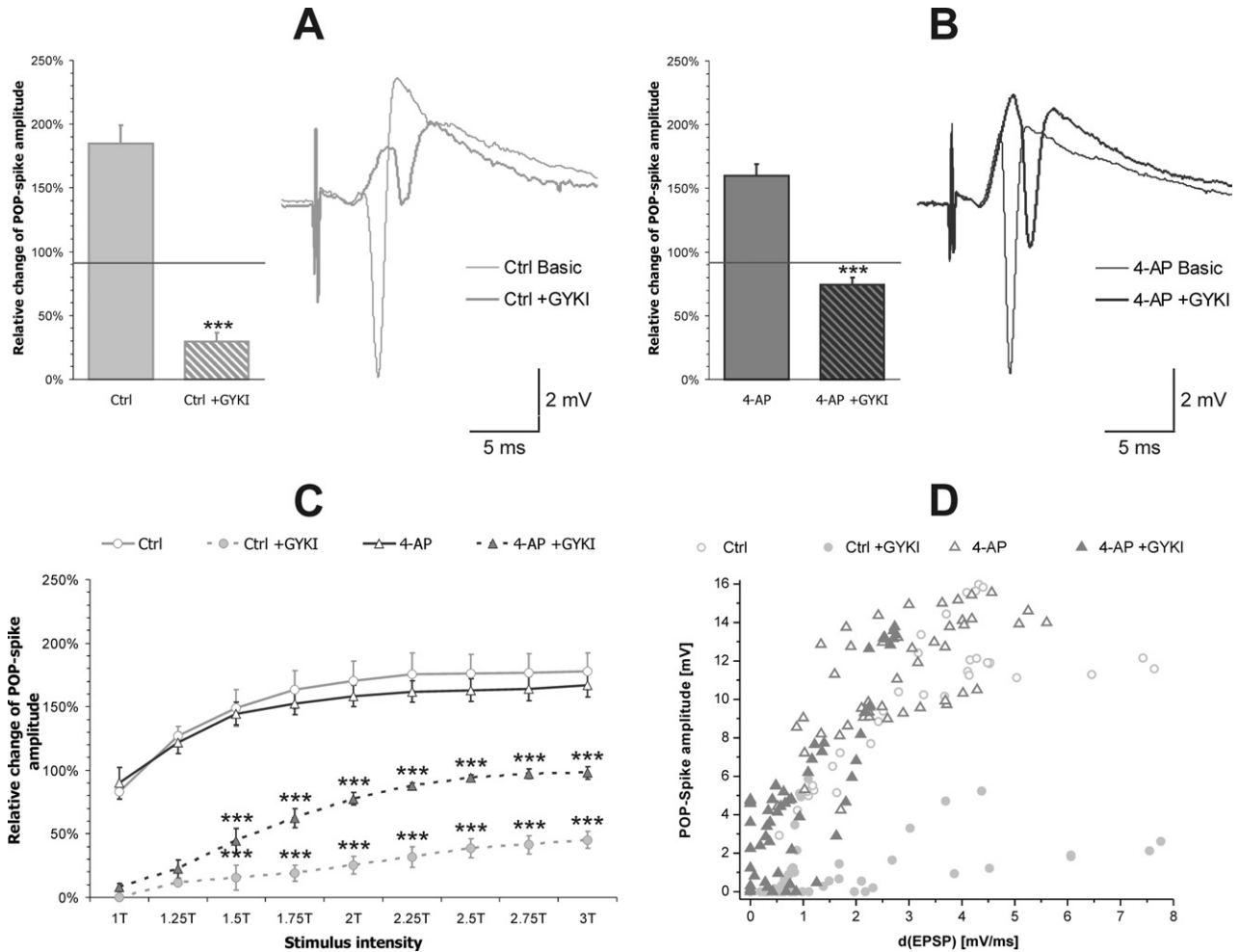
Fig. 4. Antagonistic effect of GYKI 52466 in control and 4-AP-treated rats. Forty micromolar GYKI 52466 showed a strong inhibitory effect in the control group (A) and a mild suppression in the 4-AP group (B). Both treatment groups showed a pronounced facilitation without GYKI 52466. Comparing the inhibitory effect in control and 4-AP-treated animals, data revealed a significant difference ($P=0.0214$). The reduced effectiveness of the antagonist in the 4-AP-treated group is represented with I–O curves (C) *** Indicates significant changes of POP-spike amplitude in due to GYKI 52466 compared to its control value. A strong E/S depression (right shift) can be revealed on the E/S curve (D) in the control group due to GYKI 52466, while a general decrease of POP-spike amplitude and slope of EPSP was observed in the 4-AP group after treatment with the antagonist. *** Indicates significant differences at $P<0.001$.

plitude (*** $P=0.00026$) and the slope of EPSP ($P=0.012*$) was observed, supposing the general decrease of excitability (Fig. 4D).

Statistical analysis of the changes due to APV application did not show any difference between the two experimental groups of animals. General excitability at a stimulus intensity of 2 T in the slices from control animals was 92%±1.8% ($n=8$; Fig. 5), which increased to 151%±6.9% ($n=8$) after 10 minutes. APV treatment resulted in reduced facilitation to 129%±13.5% ($n=8$). In slices of 4-AP-treated rats, the average POP-spike amplitude was 92%±0.9% ($n=8$) at the beginning of experiments and 135±7.6% ($n=8$) after 10 minutes in the normal ACSF, which increased only to 120±5.5% ($n=8$) in the presence of the NMDA receptor antagonist (Fig. 5A, B). The dynamics of synaptic transmission saturation and E/S characteristics were hardly affected (Fig. 5C, D). APV treatment did not result in significant changes.

DISCUSSION

Main findings of this study are that repeated seizures, evoked by 4-AP applications, increased the general excitability of the hippocampus and reduced the effectiveness of a non-competitive AMPA receptor antagonist, while functional properties of the NMDA receptor remained unchanged. The KA-induced Co^{2+} uptake increased in the CA1 region and in the dentate gyrus, with no change in the CA3 area, which refers to increased Ca^{2+}-influx into neurons through the rearranged AMPAR. Histoblot measurements revealed upregulation of GluR1, GluR1$_{flop}$ and NR2A glutamate receptor subunit expression in almost every investigated region of the hippocampus. However, no changes were obtained in NR1 or NR2B subunit densities. In contrast, GluR2 was downregulated in the CA1 and dentate gyrus, without corresponding changes in the CA3 region. The KA-2 subunit displayed
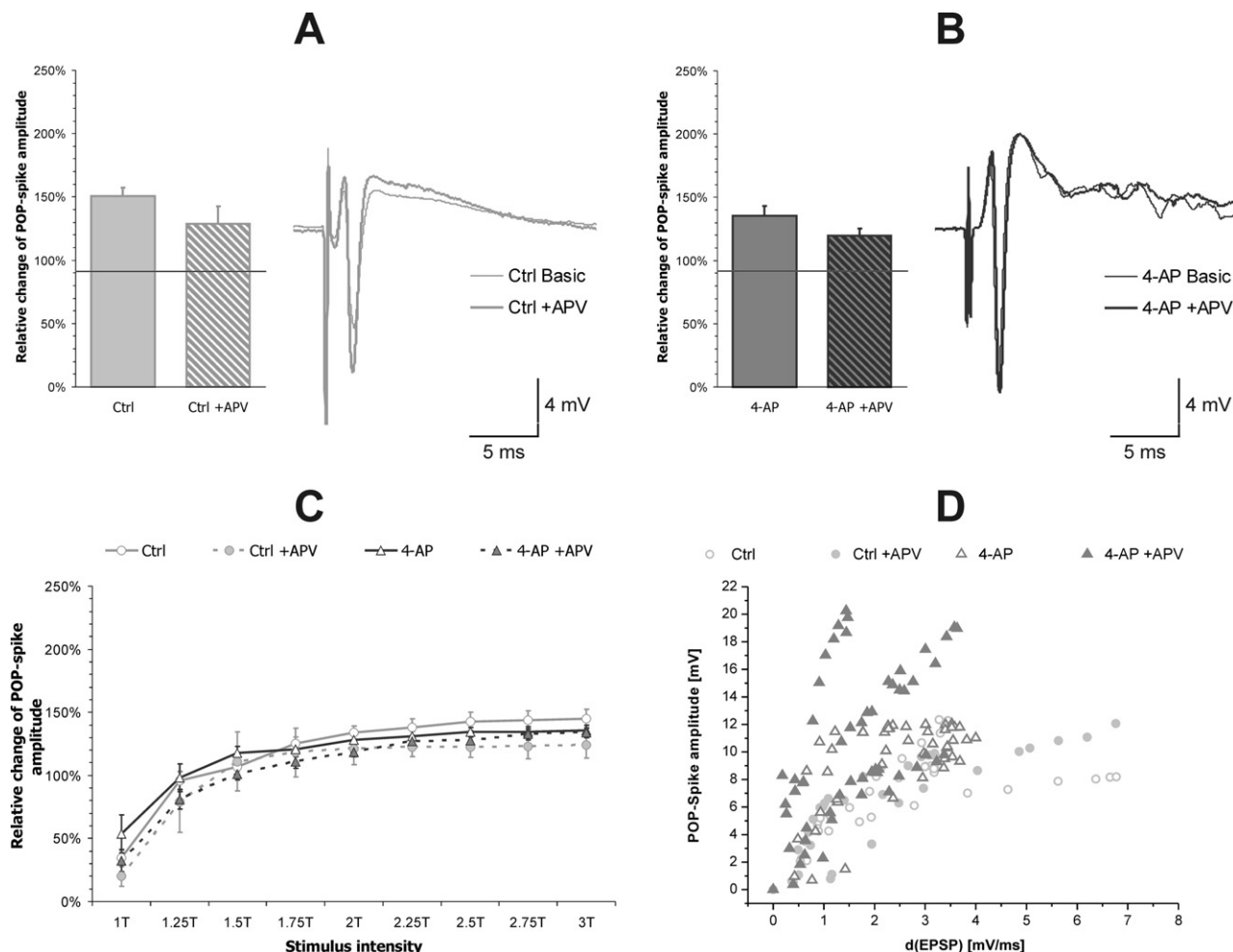
Fig. 5. Effect of APV treatment on POP-spike amplitude. Ten minutes' perfusion with 25 μM APV resulted in no change of evoked POP-spike amplitude in both groups of animals (A, B). The dynamics of saturation also remained unchanged according to I–O curves (C), in both treatment groups due to APV. Distinct separation of treatment groups can be revealed on the E/S curve (D), mild right shift can be observed.

significantly reduced staining intensity in stratum lucidum of CA3.

The effect of 4-AP

The potassium channel blocker 4-AP applied in this study is widely used as a convulsant both in *in vivo* and *in vitro* experiments. Its short-term effects are described in detail in several studies (Fragoso-Veloz et al., 1990; Hoffman et al., 1994; Versteeg et al., 1995), however, long lasting consequences are poorly investigated. Our previous studies indicated that the 4-AP model can reliably be used for the pharmacological investigation of the genesis and spread of seizures in forebrain structures *in vivo* (Mihály et al., 1997, 1998, 2001). Other chemical agents, such as KA (Nadler et al., 1978) or pilocarpine (Turski et al., 1983) also elicit convulsive events, which lead to secondarily generalized, self-sustaining seizures after a few-weeks-long seizure-free period. Common features in convulsant effects of KA and pilocarpine are the excessive release of glutamate (Cavalheiro et al., 2005) and elevated intracellular Ca^{2+} level, leading to neurodegenerative processes in hip-

pocampus and eliciting mossy fiber sprouting in dentate gyrus (Mello et al., 1993; Nadler et al., 1980). 4-AP, which also enhances presynaptic release of glutamate (Kovacs et al., 2003) and the rise of intracellular Ca^{2+} concentration, does not induce severe neurodegeneration in the abovementioned doses. Direct, intrahippocampal administration of 4-AP however, can initiate neurodegenerative processes following recurring high-frequency seizure events (Ayala and Tapia, 2005). The 2,3-benzodiazepine compound GYKI 52466 was first described as a specific AMPA receptor antagonist (Tarnawa et al., 1990) and its anticonvulsant and neuroprotective effects are well documented in different animal models. GYKI 52466 suppresses electrically induced cortical afterdischarges (Kubova et al., 1997; Világi et al., 2002) and 4-AP-induced seizures (Dóczi et al., 1999; Yamaguchi et al., 1993). The antiepileptic effect of high affinity NMDA receptor antagonist APV was demonstrated in different animal models. Oscillatory field response was suppressed by APV in disinhibited brain slice preparation (Luhmann and Prince, 1990), and the spontaneous epileptiform activity induced

by convulsants was also effectively blocked (Gulyás-Kovács et al., 2002).

Alterations of NMDA receptor subunits and function

NMDA receptors are heteromers, mainly composed of NR1 and NR2A-D subunits. The importance of NR2A and NR2B subtypes in epileptogenesis is controversial. Perinatal administration of KA induced upregulation of NR1 and NR2B expression in layer V cells of the neocortex, and the reduction of seizure threshold (Gashi et al., 2007). On the other hand, KA treatment caused seizure tolerance in hippocampal neurons (Liu et al., 2004). Repeated pilocarpine-induced status epilepticus elicited the downregulation of NR2A and NR2B subunits in the first postnatal week followed by epilepsy in later life (Silva et al., 2005). In our present experiments repeated seizures induced a significant increase in NR2A subunit density. It was reported that the NR2A subunit has more rapid kinetics compared with NR2B (Sheng et al., 1994). The NR1/NR2A subunit combination allows higher channel-opening probability and higher affinity to glutamate (Schotanus and Chergui, 2008). But, NR2A also depresses synaptic transmission in the striatum (Schotanus and Chergui, 2008). This depressant effect may depend on adenosine release which decreases presynaptic activity (Schotanus and Chergui, 2008). Susceptibility to glutamate-induced neuronal death depends on the expression of NR2A, but not of NR2B subtypes which is observed in aging neuronal cultures (Brewer et al., 2007). The fact, that NR2A increase was detected in all synaptic layers of the hippocampus following daily seizures, may underlie the general excitability increase detected in our slice experiments. Since there was no difference in the efficacy of APV in the 4-AP-treated and control slices, we can conclude that the up-regulation of NR2A subunit has no detectable effect on the pharmacological properties of the NMDA receptor. The long-term significance of this alteration is unclear: it may increase cellular vulnerability (Brewer et al., 2007).

Alterations of AMPA receptor subunits and function

AMPA receptors are heterotetramers of GluR1-4 subunits. Neurons in the forebrain, including the hippocampus predominantly express GluR1/GluR2 subunit-containing heterotetramers (Geiger et al., 1995). The Q/R-edited GluR2 subunit has a key role in the determination of AMPAR Ca^{2+} permeability, receptor kinetics, single channel conductance and blockade by endogenous polyamines therefore its expression is strictly regulated (Isaac et al., 2007). Relative reduction in GluR2 expression likely increases Ca^{2+} permeability of AMPARs in neurons (Pellegrini-Giampietro et al., 1997). Our histoblot experiments revealed a reduction in total AMPAR (GluR1-4) subunit levels with relative upregulation of GluR1 and GluR1$_{flop}$ subunits and the corresponding downregulation of GluR2 in the synaptic layers of CA1 and dentate gyrus, which may lead to the formation of GluR2 lacking AMPARs with increased Ca^{2+} permeability. Furthermore, our Co^{2+} uptake measurements confirmed the increase in Ca^{2+} uptake in the CA1 area and in the dentate gyrus, which is consistent with the

results of the histoblot analysis. A more pronounced down-regulation of GluR2 subtype was observed in chronic KA induced epilepsy models (Friedman et al., 1994), leading to neurodegeneration in different hippocampal areas (Nadler et al., 1978; Turski et al., 1983). Decreased effects of the AMPAR antagonist GYKI 52466 in 4-AP-treated animals also indicate changes in AMPAR composition. This could also be explained with the downregulation of GluR2 expression. GYKI 52466 is less potent at homomeric GluR1 and GluR4 receptors compare with GluR2-containing heteromeric AMPARs (Johansen et al., 1995; Bleakman et al., 1996). While homomeric GluR6 and heteromeric GluR6/KA-2 KA receptors are also influenced by GYKI 52466, the effective concentration is much higher than what was applied in our study (Bleakman et al., 1996; Yamada and Turetsky, 1996). Glutamate-induced currents in hippocampal neurons which possess heteromeric AMPARs were effectively blocked by low concentration of GYKI 52466, but KA-induced currents in GluR5/KA-2 expressing dorsal root ganglion cells were hardly inhibited (Yamada and Turetsky, 1996). Therefore the observed reduction in GYKI 52466 sensitivity is consistent with the appearance of GluR2-lacking AMPARs.

Despite the downregulation of GluR2, no neuronal loss was observed. In ischemia or KA-induced status epilepticus, downregulation of the GluR2 subunit is rapid and much more pronounced (>50%–60%) and often leads to the loss of neurons via excitotoxicity (Pellegrini-Giampietro et al., 1997). The increase in Ca^{2+} permeability can lead to the rise of conductivity of the AMPARs, which can also explain the reduced potency of GYKI 52466 in 4-AP-treated slices. The POP-spike in the CA1 region can be effectively suppressed in control slices by GYKI 52466 similarly to that reported previously (Marinelli et al., 2000). However, the antagonist was less potent in 4-AP-treated slices. Interestingly, recent *in vivo* experiments from our laboratory proved, that GYKI 52466 was completely ineffective in preventing the convulsion-related astrocytic swelling in the hippocampus (Weiczner et al., 2008). Collectively, these findings support the notion that GluR2-lacking, Ca^{2+}-permeable AMPARs appear following 4-AP seizures.

KA receptor alterations

KA receptors have five different subunits: GluR5-7, KA-1 and KA-2 (Huettner, 2003). Our histoblot measurements revealed the downregulation of KA-2 subunit in stratum lucidum of the CA3 area. High densities of KA receptors were found at the mossy fiber–CA3 pyramidal cell synapse (Wisden and Seeburg, 1993). Since the KA-2 subunit is more abundant in the postsynaptic region (Darstein et al., 2003), we can assume that the observed downregulation of this subunit in our experiments reflects postsynaptic changes. There was no corresponding reduction in Co^{2+} uptake in stratum lucidum of the CA3 region, which may be due to compensatory changes in other KA receptor subunits not investigated in our study or limited sensitivity of the Co^{2+} uptake method. The KA receptor is associated

with mossy fibers, therefore we can conclude, that no mossy fiber sprouting did occur in our seizure experiments.

CONCLUSIONS

The rearrangement of iGluRs increased the general neuronal excitability of the hippocampus without neurodegenerative symptoms. The alteration indicated the lack of mossy fiber sprouting following repeated 4-AP seizures. The results suggest that repeated short convulsions result in plastic changes in the molecular composition of iGluRs. The altered receptors may increase the calcium permeability of hippocampal neurons. These long-lasting changes likely increase the excitability of the hippocampus, however, the direction of alterations might be different in other cortical areas. Further experiments are needed to support this final conclusion.

REFERENCES

Ayala GX, Tapia R (2005) Late *N*-methyl-D-aspartate receptor blockade rescues hippocampal neurons from excitotoxic stress and death after 4-aminopyridine-induced epilepsy. Eur J Neurosci 22:3067–3076.

Berg M, Bruhn T, Johansen FF, Diemer NH (1993) Kainic acid-induced seizures and brain damage in the rat: different effects of NMDA and AMPA receptor agonists. Pharmacol Toxicol 73:262–268.

Bleakman D, Ballyk BA, Schoepp DD, Palmer AJ, Bath CP, Sharpe EF, Woolley ML, Bufton HR, Kamboj RK, Tarnawa I, Lodge D (1996) Activity of 2,3-benzodiazepines at native rat and recombinant human glutamate receptors in vitro: stereospecificity and selectivity profiles. Neuropharmacology 35:1689–1702.

Brewer LD, Thibault O, Staton J, Thibault V, Rogers JT, Garcia-Ramos G, Kraner S, Landfield PW, Porter NM (2007) Increased vulnerability of hippocampal neurons with age in culture: temporal association with increases in NMDA receptor current, NR2A subunit expression and recruitment of L-type calcium channels. Brain Res 1151:20–31.

Cavalheiro E, Naffah-Mazzacoratti M, Mello L, Leite J, Pitkanen A, Schwartzkroin P, Moshe S (2005) The pilocarpine model of seizures, pp 433–448. Academic Press.

Cavalheiro EA (1995) The pilocarpine model of epilepsy. Ital J Neurol Sci 16:33–37.

Darstein M, Petralia RS, Swanson GT, Wenthold RJ, Heinemann SF (2003) Distribution of kainate receptor subunits at hippocampal mossy fiber synapses. J Neurosci 23:8013–8019.

Dóczi J, Banczerowski-Pelyhe I, Barna B, Vilagi I (1999) Effect of a glutamate receptor antagonist (GYKI 52,466) on 4-aminopyridine-induced seizure activity developed in rat cortical slices. Brain Res Bull 49:435–440.

Fabene PF, Weiczner R, Marzola P, Nicolato E, Calderan L, Andrioli A, Farkas E, Sule Z, Mihaly A, Sbarbati A (2006) Structural and functional MRI following 4-aminopyridine-induced seizures: a comparative imaging and anatomical study. Neurobiol Dis 21:80–89.

Fragoso-Veloz J, Massieu L, Alvarado R, Tapia R (1990) Seizures and wet-dog shakes induced by 4-aminopyridine, and their potentiation by nifedipine. Eur J Pharmacol 178:275–284.

Friedman LK, Pellegrini-Giampietro DE, Sperber EF, Bennett MV, Moshe SL, Zukin RS (1994) Kainate-induced status epilepticus alters glutamate and GABA$_A$ receptor gene expression in adult rat hippocampus: an in situ hybridization study. J Neurosci 14: 2697–2707.

Gashi E, Avallone J, Webster T, Friedman LK (2007) Altered excitability and distribution of NMDA receptor subunit proteins in cortical layers of rat pups following multiple perinatal seizures. Brain Res 1145:56–65.

Geiger JR, Melcher T, Koh DS, Sakmann B, Seeburg PH, Jonas P, Monyer H (1995) Relative abundance of subunit mRNAs determines gating and Ca2+ permeability of AMPA receptors in principal neurons and interneurons in rat CNS. Neuron 15:193–204.

Gulyás-Kovács A, Doczi J, Tarnawa I, Detari L, Banczerowski-Pelyhe I, Vilagi I (2002) Comparison of spontaneous and evoked epileptiform activity in three in vitro epilepsy models. Brain Res 945: 174–180.

Hassel B, Dingledine R (2006) Glutamate, pp 267–290. Academic Press.

Hoffman SN, Saline PA, Prince DA (1994) chronic neocortical epileptogenesis in vitro. J Neurophysiol 71:1762–1773.

Honavar M, Meldrum B, Graham D, Lantos P (2002) Epilepsy, pp 899–941. London: Arnold.

Huettner JE (2003) Kainate receptors and synaptic transmission. Prog Neurobiol 70:387–407.

Isaac JT, Ashby M, McBain CJ (2007) The role of the GluR2 subunit in AMPA receptor function and synaptic plasticity. Neuron 54:859–871.

Johansen TH, Chaudhary A, Verdoorn TA (1995) Interactions among GYKI-52466, cyclothiazide, and aniracetam at recombinant AMPA and kainate receptors. Mol Pharmacol 48:946–955.

Kopniczky Z, Dobo E, Borbely S, Vilagi I, Detari L, Krisztin-Peva B, Bagosi A, Molnar E, Mihaly A (2005) Lateral entorhinal cortex lesions rearrange afferents, glutamate receptors, increase seizure latency and suppress seizure-induced c-fos expression in the hippocampus of adult rat. J Neurochem 95:111–124.

Kovacs A, Mihaly A, Komaromi A, Gyengesi E, Szente M, Weiczner R, Krisztin-Peva B, Szabo G, Telegdy G (2003) Seizure, neurotransmitter release, and gene expression are closely related in the striatum of 4-aminopyridine-treated rats. Epilepsy Res 55:117–129.

Kubova H, Vilagi I, Mikulecka A, Mares P (1997) Non-NMDA receptor antagonist GYKI 52,466 suppresses cortical afterdischarges in immature rats. Eur J Pharmacol 333:17–26.

Liu S, Lau L, Wei J, Zhu D, Zou S, Sun HS, Fu Y, Liu F, Lu Y (2004) Expression of Ca(2+)-permeable AMPA receptor channels primes cell death in transient forebrain ischemia. Neuron 43:43–55.

Luhmann HJ, Prince DA (1990) Control of NMDA receptor-mediated activity by GABAergic mechanisms in mature and developing rat neocortex. Brain Res Dev Brain Res 54:287–290.

Marinelli S, Gatta F, Sagratella S (2000) Effects of GYKI 52,466 and some 2,3-benzodiazepine derivatives on hippocampal in vitro basal neuronal excitability and 4-aminopyridine epileptic activity. Eur J Pharmacol 391:75–80.

Meldrum BS, Nilsson B (1976) Cerebral blood flow and metabolic rate early and late in prolonged epileptic seizures induced in rats by bicuculline. Brain 99:523–542.

Mello LE, Cavalheiro EA, Tan AM, Kupfer WR, Pretorius JK, Babb TL, Finch DM (1993) Circuit mechanisms of seizures in the pilocarpine model of chronic epilepsy: cell loss and mossy fiber sprouting. Epilepsia 34:985–995.

Michaelis EK (1998) Molecular biology of glutamate receptors in the central nervous system and their role in excitotoxicity, oxidative stress and aging. Prog Neurobiol 54:369–415.

Mihály A, Bencsik K, Solymosi T (1990) Naltrexone potentiates 4-aminopyridine seizures in the rat. J Neural Transm Gen Sect 79: 59–67.

Mihály A, Shihab-Eldeen A, Owunwanne A, Gopinath S, Ayesha A, Mathew M (2000) Acute 4-aminopyridine seizures increase the regional cerebral blood flow in the thalamus and neocortex, but not in the entire allocortex of the mouse brain. Acta Physiol Hung 87:43–52.

Mihaly A, Szakacs R, Bohata C, Dobo E, Krisztin-Peva B (2001) Time-dependent distribution and neuronal localization of c-fos protein in the rat hippocampus following 4-aminopyridine seizures. Epilepsy Res 44:97–108.

Mihaly A, Szente M, Dobo E, Por I (1998) Early activation of inhibitory neurons in the thalamic reticular nucleus during focal neocortical seizures. Acta Histochem 100:383–393.

Mihály A, Szente M, Dubravcsik Z, Boda B, Kiraly E, Nagy T, Domonkos A (1997) Parvalbumin- and calbindin-containing neurons express c-fos protein in primary and secondary (mirror) epileptic foci of the rat neocortex. Brain Res 761:135–145.

Nadler JV, Perry BW, Cotman CW (1978) Intraventricular kainic acid preferentially destroys hippocampal pyramidal cells. Nature 271:676–677.

Nadler JV, Perry BW, Cotman CW (1980) Selective reinnervation of hippocampal area CA1 and the fascia dentata after destruction of CA3-CA4 afferents with kainic acid. Brain Res 182:1–9.

Pellegrini-Giampietro DE, Gorter JA, Bennett MV, Zukin RS (1997) The GluR2 (GluR-B) hypothesis: Ca(2+)-permeable AMPA receptors in neurological disorders. Trends Neurosci 20:464–470.

Pena F, Tapia R (2000) Seizures and neurodegeneration induced by 4-aminopyridine in rat hippocampus in vivo: role of glutamate- and GABA-mediated neurotransmission and of ion channels. Neuroscience 101:547–561.

Pickard L, Noel J, Henley JM, Collingridge GL, Molnar E (2000) Developmental changes in synaptic AMPA and NMDA receptor distribution and AMPA receptor subunit composition in living hippocampal neurons. J Neurosci 20:7922–7931.

Porter BE, Cui XN, Brooks-Kayal AR (2006) Status epilepticus differentially alters AMPA and kainate receptor subunit expression in mature and immature dentate granule neurons. Eur J Neurosci 23:2857–2863.

Pruss RM, Akeson RL, Racke MM, Wilburn JL (1991) Agonist-activated cobalt uptake identifies divalent cation-permeable kainate receptors on neurons and glial cells. Neuron 7:509–518.

Racine RJ (1972) Modification of seizure activity by electrical stimulation. II. Motor seizurez. Electroencephalogr Clin Neurophysiol 32:281–294.

Schotanus SM, Chergui K (2008) NR2A-containing NMDA receptors depress glutamatergic synaptic transmission and evoked-dopamine release in the mouse striatum. J Neurochem 106:1758–1765.

Sheng M, Cummings J, Roldan LA, Jan YN, Jan LY (1994) Changing subunit composition of heteromeric NMDA receptors during development of rat cortex. Nature 368:144–147.

Silva AV, Regondi MC, Cipelletti B, Frassoni C, Cavalheiro EA, Spreafico R (2005) Neocortical and hippocampal changes after multiple pilocarpine-induced status epilepticus in rats. Epilepsia 46:636–642.

Singh L, Oles RJ, Vass CA, Woodruff GN (1991) A slow intravenous infusion of N-methyl-DL-aspartate as a seizure model in the mouse. J Neurosci Methods 37:227–232.

Sloviter RS, Dempster DW (1985) "Epileptic" brain damage is replicated qualitatively in the rat hippocampus by central injection of glutamate or aspartate but not by GABA or acetylcholine. Brain Res Bull 15:39–60.

Szakács R, Weiczner R, Mihaly A, Krisztin-Peva B, Zador Z, Zador E (2003) Non-competitive NMDA receptor antagonists moderate seizure-induced c-fos expression in the rat cerebral cortex. Brain Res Bull 59:485–493.

Tarnawa I, Engberg I, Flatman J, Lubec G, Rosenthal G (1990) GYKI 52,466, an inhibitor of spinal reflexes is a potent quisqualate antagonist. In: ESCOM, pp 538–546. Leiden: Science Press.

Tonnes J, Stierli B, Cerletti C, Behrmann JT, Molnar E, Streit P (1999) Regional distribution and developmental changes of GluR1-flop protein revealed by monoclonal antibody in rat brain. J Neurochem 73:2195–2205.

Turski WA, Cavalheiro EA, Schwarz M, Czuczwar SJ, Kleinrok Z, Turski L (1983) Limbic seizures produced by pilocarpine in rats: behavioural, electroencephalographic and neuropathological study. Behav Brain Res 9:315–335.

Versteeg DH, Heemskerk FM, Spierenburg HA, de Graan PN, Schrama LH (1995) 4-Aminopyridine differentially affects the spontaneous release of radiolabelled transmitters from rat brain slices in vitro. Brain Res 686:233–238.

Világi I, Takacs J, Gulyas-Kovacs A, Banczerowski-Pelyhe I, Tarnawa I (2002) Protective effect of the antiepileptic drug candidate talampanel against AMPA-induced striatal neurotoxicity in neonatal rats. Brain Res Bull 59:35–40.

Vizi S, Bagosi A, Krisztin-Peva B, Gulya K, Mihaly A (2004) Repeated 4-aminopyridine seizures reduce parvalbumin content in the medial mammillary nucleus of the rat brain. Brain Res Mol Br Res 131:110–118.

Weiczner R, Krisztin-Peva B, Mihaly A (2008) Blockade of AMPA-receptors attenuates 4-aminopyridine seizures, decreases the activation of inhibitory neurons but is ineffective against seizure-related astrocytic swelling. Epilepsy Res 78:22–32.

Wheal HV, Bernard C, Chad JE, Cannon RC (1998) Pro-epileptic changes in synaptic function can be accompanied by pro-epileptic changes in neuronal excitability. Trends Neurosci 21:167–174.

Wisden W, Seeburg PH (1993) A complex mosaic of high-affinity kainate receptors in rat brain. J Neurosci 13:3582–3598.

Xu B, McIntyre DC, Fahnestock M, Racine RJ (2004) Strain differences affect the induction of status epilepticus and seizure-induced morphological changes. Eur J Neurosci 20:403–418.

Yamada KA, Turetsky DM (1996) Allosteric interactions between cyclothiazide and AMPA/kainate receptor antagonists. Br J Pharmacol 117:1663–1672.

Yamaguchi S, Donevan SD, Rogawski MA (1993) Anticonvulsant activity of AMPA/kainate antagonists: comparison of GYKI 52,466 and NBOX in maximal electroshock and chemoconvulsant seizure models. Epilepsy Res 15:179–184.

(Available online 27 December 2008)